Available online at www.sciencedirect.com
SCIENCE DIRECT®
International Journal of Thermal Sciences 41 (2002) 1067–1075
International Journal of Thermal Sciences
www.elsevier.com/locate/ijts

Convective heat transport along a thermoacoustic couple in the transient regime

Antonio Piccolo *, Giuseppe Cannistraro

Dipartimento di Fisica, Facoltà di Ingegnerià, Universita degli Studi di Messina, Contrada Papardo, Salita Sperone 31, P.O. Box 55, 98166 S. Agata (Messina), Italy

Received 10 May 2001; accepted 10 December 2001

Abstract

This work proposes a simple calculus procedure based on the linear thermoacoustic theory. The methodology applies on rate of change (time derivative) rather than on steady state temperature distributions so it constitutes a complementary to conventional analysis to perform test on the reliability and applicability of the linear theory. The procedure has been applied to experimental data collected by means of a simple prototype of thermoacoustic device. The apparatus, whose technical characteristics are described in detail along with the data acquisition procedure, has been able to highlight the general features of the thermoacoustic effect. Measurements concern the acoustically generated temperature gradients across a ThermoAcoustic Couple, a structure firstly introduced by Wheatley and coworkers in 1983. The obtained results indicate that heat transfer phenomena are more critical than non linear acoustic behavior in determining the overestimation that theoretical predictions make on experimental values.

Keywords: Thermoacoustics; Prime movers; Refrigerators; Heat pumps; Heat; Sound

1. Introduction

Thermoacoustics describes energy conversion processes activated by the interaction of the temperature oscillation accompanying the pressure oscillation in a sound wave with solid boundaries. In ordinary experience this interaction of sound and heat cannot be observed, being very low the temperature differences involved, but, under suitable conditions, it can be emphasized and amplified to give rise to remarkable thermodynamic effects such as steep thermal gradients, powerful convective heat fluxes, strong sound fields.

Since 1850 Sondhaus [1] noticed that when a hot glass bulb was attached to a cool glass tubular stem it emitted sound. The complementary effect was pointed out, among others, by Merkli and Thomann [2] who in 1972 observed a cooling effect near the velocity antinode of an acoustically resonating tube closed at one end and driven at the other end by an oscillating piston. The first qualitative explanation of the phenomenon was given in 1896 by Rayleigh [3] who emphasized the importance of the time phasing between temperature and fluid particle motion. But only in 1969 Rott [4] formulated a quantitative first order (linear) theory, subsequently developed and refined by Swift [5].

Nowadays, thermoacoustic devices have reached a good level of advancement and seem to have the immediate potential to be used as alternative to conventional energy-conversion systems that are in widespread use such as the internal combustion engine, the steam turbine, the vapour-compression refrigerator, the gas turbine, etc. Thermoacoustic engines, in fact, have the advantage of a complete absence of moving mechanical parts and operate using environmentally no-harmful working fluids so they hold out the possibility of extreme simplicity and reliability. These characteristics, in turn, could lead to low manufacturing and maintenance costs. Relevant prototypes are the pioneer Hofler's thermoacoustic refrigerator [6], the liquid sodium [7,8] and 13.8 bar helium filled [9] acoustic prime movers, the SETAC [10] and STAR [11] thermoacoustic refrigerators, the multipurpose life sciences cooler TALSR [12] capable of producing 419 W of cooling power or the TADOPTR unit [13,14] (a natural and industrial gas liquefier) having a liquefying capacity of about 600 liter per day and which uses a natural gas burner as power source.

* Corresponding author.
E-mail address: apiccolo@unime.it (A. Piccolo).

1290-0729/02/$ – see front matter
PII: S1290-0729(02)01393-5

Nomenclature

a	speed of sound	$m \cdot s^{-1}$
c_A	specific heat per unit area of a stack plate	$J \cdot m^{-2} \cdot K^{-1}$
c_P	isobaric specific heat of the working fluid	$J \cdot kg^{-1} \cdot K^{-1}$
c_S	specific heat of the stack plates	$J \cdot kg^{-1} \cdot K^{-1}$
C	"cold" side of the stack	
DR	$= P_A/P_m$ drive ratio	
f_ν	Rott's function	
$\dot{H}_2$	enthalpy flux	W
H	"hot" side of the stack	
i	imaginary unit	
k^*	complex wave number	m^{-1}
K	thermal conductivity of the working fluid	$W \cdot m^{-1} \cdot K^{-1}$
K_S	thermal conductivity of the stack plates	$W \cdot m^{-1} \cdot K^{-1}$
l	half of the plate thickness	m
L	resonator length	m
P_A	amplitude of the dynamic pressure at the driver-end	Pa
P_m	mean pressure	Pa
P_1	local amplitude of the dynamic pressure	Pa
$\dot{q}_2$	heat flux extracted from C per unit area of plate	$W \cdot m^{-2}$
$(\dot{q}_2)_0$	initial time heat flux extracted from C per unit area of plate	$W \cdot m^{-2}$
$\dot{Q}_2$	heat flux	W
$(\dot{Q}_2)_0$	initial time heat flux	W
Re	Reynolds number	
t	time	s
T_C	local temperature in C	K
T_H	local temperature in H	K
T_m	mean temperature	K
T_1	local amplitude of the acoustic temperature oscillations	K
U_A	amplitude of the acoustic particle velocity at the driver-end	$m \cdot s^{-1}$
u_1	local amplitude of the acoustic particle velocity	$m \cdot s^{-1}$
x	axial coordinate	m
X	x axis	
y	transverse coordinate	m
y_o	half distance between two plates	m
Y	y axis	
$\dot{W}_2$	acoustic power	W

Greek symbols

α	sound absorption coefficient	m^{-1}
β	thermal expansion coefficient of the working fluid	K^{-1}
β'	phase constant	m^{-1}
γ	ratio of the isobaric to isochoric specific heat	
γ'	propagation constant	$m^{-1}]$
δ_S	thermal penetration depth of a stack plate	m
δ_κ	thermal penetration depth of the working fluid	m
δ_ν	viscous penetration depth of the working fluid	m
Δx	stack length along the X direction	m
ΔT	$= (T_H - T_C)$ temperature difference	K
ε_S	stack heat capacity correction factor	
λ	wavelength	m
ν	kinematic viscosity	$m^2 \cdot s^{-1}$
ξ	$= (L - x)$ mean distance of the stack from the driver	m
Π	transverse perimeter of a stack-plate	m
ρ_m	mean density of the working fluid	$kg \cdot m^{-3}$
ρ_S	density of the stack-plates	$kg \cdot m^{-3}$
σ	Prandtl number	
ω	angular frequency	$rad \cdot s^{-1}$

Subscripts

0	initial time value
1, 2, ...	first, second, ... order acoustic variable
A	per unit area value, acoustic amplitude at the driver-end
C	value referred to the cold side of a plate
H	value referred to the hot side of a plate
m	mean
P	isobaric
s	solid stack
x	x component
κ	thermal
ν	viscous

Although the efficiencies of prototypes are improving they are at twenty to thirty percent of Carnot efficiency, still below those of conventional technologies. The estimates of the performances of these engines are actually obtained from the linear theory of thermoacoustics. It is generally found that the measured performances are consistent with linear analysis only at low values of the drive ratio DR (the ratio of the acoustic pressure amplitude in a pressure antinode, P_A, to the mean pressure of the fluid, P_m). At high pressure amplitudes (for $DR = P_A/P_m \geqslant 0.003$) the calculated thermal and acoustic quantities systematically overestimate the measured ones by twenty, thirty and in some cases also by fifty percent [9, 15–17]. From a practical point of view these deviations are deleterious because are associated with a decrease in efficiency.

On the other hand, in the perspective of widespread commercial applications of thermoacoustic engines, the design of even more efficient apparatus requires an understanding of the origin of such deviations for the sake of obtaining reliable theoretical predictions at moderate and large dynamic pressure amplitudes.

An important matter is then to point out an eventual sudden onset for the deviations from the behavior expected by the linear theory as well as to establish if the origin of such deviations is imputable to complex non-linear processes [18] or to heat transfer phenomena [19–21] which are not taken into account by the standard theory.

In such contexts, this work proposes a simple calculus procedure which could help to investigate on the above formulated issues. The methodology, based on the linear theory, applies on rate of change (time derivative) rather than on steady state temperature distributions. In particular, the derivatives can be taken at the start-up (initial time) of the devices when temperature is uniform through all the system and no (time-average) thermal exchanges can take place among different components of the system or between the system and its surrounding. In this way, the influence of heat transfer problems (not included in the standard theory) on the experimental data is naturally eliminated (or minimized) and eventual deviations from the linear theory have to be attributed to other causes such as non-linear acoustic behavior, turbulent flux, etc.

Unfortunately, the experimental data to be found in literature refer to devices operating in steady-state conditions and do not include temporal measurements relative to the transient regime of approach to the dynamic equilibrium to which our calculus procedure applies. For this reason, in the present work an experimental study on the thermoacoustic effect has been carried out making use of structures and apparatus the simplest as possible in order to facilitate the interpretation of the experimental results.

The thermoacoustic device assembled is based on the so called "ThermoAcoustic Couple" (TAC) firstly introduced by Wheatley and coworkers [22–24] in 1983 and further adopted by other researchers [15,21]. The time evolution of the temperature gradients induced across the TAC by an acoustic standing wave has been measured as a function of the TAC position relative to the acoustic field and of the drive ratio. The TAC, introducing a simplification of the theory underlying the thermoacoustic phenomenon allows precise quantitative analysis without complicated analytical computations.

The aim of the present work, therefore, is to illustrate an application of the calculus procedure to the experimental data collected by means of the above described prototype. At this stage, collected data fall only in the moderately high drive ratio domain ($DR \leqslant 0.011$) where deviations begin to show up and over which thermoacoustic devices generally operate.

2. Theory

An exhaustive treatment of the linear theory (first order expansion in the acoustic amplitude of all basic variables) of thermoacoustic heat transport can be found in the review article of Swift [5]. Here we only give a qualitative description of the phenomenon reporting the analytical formulas applied for the analysis of the experimental results. The notation is the same used by Swift.

When a short stack of parallel plates is properly placed inside an acoustically resonant tube, a thermal gradient rapidly develops across the plates, in the longitudinal direction X (see Figs. 1 and 2), i.e., in the direction of the particle acoustic displacement. If the stack is well thermally insulated, a limiting temperature distribution quickly results, where the "hot" side of the stack, H, is close to the nearest pressure antinode and the "cold" side, C, is close to

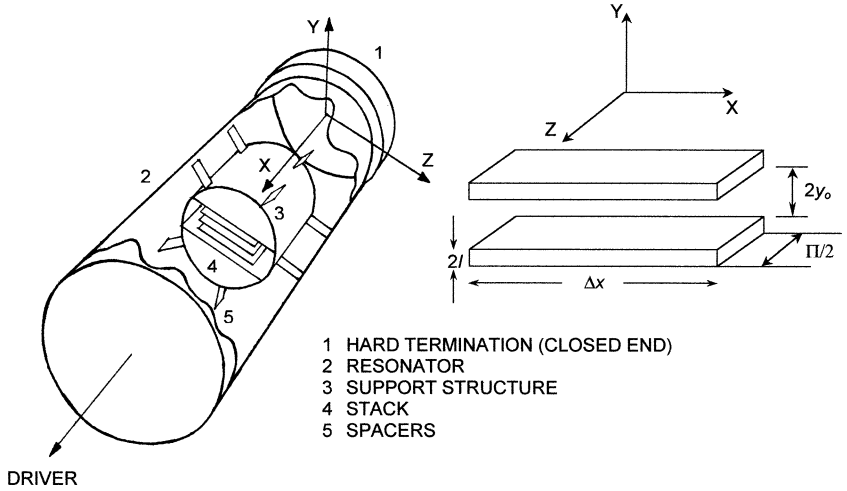

Fig. 1. Sketch of the experimental apparatus and of the stack plates geometry.

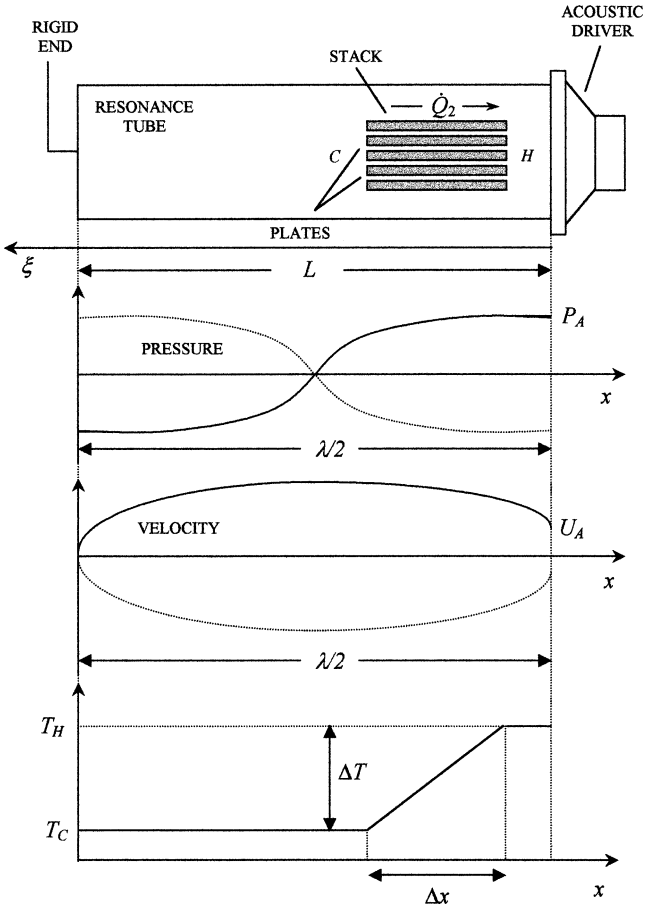

Fig. 2. Pressure velocity and temperature distributions along the resonator.

the nearest velocity antinode. The temperature difference thus obtained $\Delta T = T_H - T_C$ can greatly exceed the adiabatic gas temperature oscillations resulting from the pressure oscillations. It is well established that the origin of such an effect must be attributed to an acoustically stimulated hydrodynamic heat flow which takes place in the gas within a thermal penetration depth δ_κ from the surface of the plates and is directed from C to H. If the equilibrium thermal gradient is lower than a critical value [5] and the stack ends are supplied with heat exchangers, a heat pump is then obtained, where the work is done by the acoustic field.

The basic physical mechanism of this effect can be singled out considering that in an acoustic wave fluid particles are adiabatically expanded and compressed about their mean equilibrium positions. For particles oscillating within a distance δ_κ from the plates the thermal interaction with the solid boundary introduces a time phase lag between temperature and pressure oscillating fields (otherwise in phase). In this way, particles are forced to describe in their oscillatory motion thermodynamic cycles with non-zero areas so absorbing mechanical work from the stationary wave. At the same time, they are able to pick up heat from the plates in a low temperature point and to return it in another point at higher temperature.

Balance equations of fluid mechanics provide the following expression for the time-averaged hydrodynamic heat flow in the direction X along a plate of the stack [22]

$$\dot{Q}_2 = \Pi \int_0^{y_0} \left(\rho_m c_P \overline{T_1 u_1} - T_m \beta \overline{P_1 u_1}\right) \mathrm{d}y \tag{1}$$

where bars denote time-average over an acoustic cycle.

The integration of this equation is simplified if the stack plates satisfy the requisites of a TAC:

$(\Delta x \ll \lambda/2\pi)$ "short stack approximation"
$(\delta_\kappa, \delta_\nu \ll y_o; \delta_s \ll l)$ "boundary layer approximation".

We however do not directly integrate Eq. (1) but utilize results of Ref. [5] to find an explicit expression of $\dot{Q}_2$. Starting from the first principle of thermodynamics

$$\dot{Q}_2 = \dot{H}_2 - \dot{W}_2 \tag{2}$$

we replace the hydrodynamic enthalpy flux ($\dot{H}_2$) with the first two terms of Eq. (A.30) of Ref. [5] and the acoustic power flow ($\dot{W}_2$) with Eq. (A.32) of Ref. [5] which can be rewritten in the equivalent form

$$\dot{W}_2 = \frac{\Pi y_o}{2\omega\rho_m} \mathrm{Im}\left[P_1 \frac{\mathrm{d}\widetilde{P}_1}{\mathrm{d}x}\left(1 - \tilde{f}_\nu\right)\right] \tag{3}$$

where the Rott's function f_ν is defined as

$$f_\nu = \frac{\tanh[(1+i)y_o/\delta_\nu]}{(1+i)y_o/\delta_\nu} \tag{4}$$

and where tilde indicates complex conjugation. Moreover, we use Eq. (73) of Ref. [5] to express the derivatives $(\mathrm{d}P_1/\mathrm{d}x)$ and $(\mathrm{d}\widetilde{P}_1/\mathrm{d}x)$ in terms of $\langle u_1\rangle$ and $\langle\tilde{u}_1\rangle$. Making substitutions and applying simplifications deriving from the "short stack" and "boundary layer" approximations [5] the following relation for the time average hydrodynamic heat flow along the X direction is found:

$$\begin{aligned}\dot{Q}_2 = {} & \frac{\Pi\delta_\kappa}{4}\frac{T_m\beta}{(1+\varepsilon_s)(1+\sigma)} \\ & \times \mathrm{Im}\left\{\frac{[(1+\sqrt{\sigma})+i(1-\sqrt{\sigma})]}{[1-(1-i)\delta_\nu/2y_o]} P_1\langle\tilde{u}_1\rangle\right\} \\ & - \frac{\Pi\delta_\kappa}{4}\frac{\rho_m c_P[(1+\sigma\varepsilon_s)-\sigma\sqrt{\sigma}(1+\varepsilon_s)]}{\omega(1+\varepsilon_s)(1-\sigma^2)(1-\delta_\nu/y_o+\delta_\nu^2/2y_o^2)} \\ & \times \frac{\mathrm{d}T_m}{\mathrm{d}x}\left|\langle u_1\rangle\right|^2\end{aligned} \tag{5}$$

where $\varepsilon_S = (\sqrt{K\rho_m c_P})/(\sqrt{K_S\rho_S c_S})$ and brackets $\langle\,\rangle$ denote transverse spatial average (along the Y direction). Moreover, in Eq. (5) the sign of the first addend has been changed $(-\to+)$ to take into account the sign of P_1 and $\langle u_1\rangle$ (see Eqs. (11)). In this way, positive values of $\dot{Q}_2$ mean average heat flows toward the driver-end, i.e., toward the nearest pressure antinode, as it must result if the device is operating in the refrigeration mode.

As no thermal reservoirs are connected to the stack ends, the flow is sustained from the plates themselves. Each

plate, therefore, will cool at C, where heat is removed and will heat at H, where heat is reversed. However, as a consequence of thermal conduction in the plates and in the surrounding gas, the magnitude of the resulting thermal gradient ($\mathrm{d}T_m/\mathrm{d}x$) cannot grow indefinitely. The maximum (equilibrium) value of $\mathrm{d}T_m/\mathrm{d}x$, in fact, is achieved when $\dot{Q}_2$ is perfectly balanced by a diffusive heat flow from H to C. The balance equation for each point x along the plate is:

$$\dot{Q}_2 - \Pi(Ky_0 + K_s l)\frac{\mathrm{d}T_m}{\mathrm{d}x} = 0 \tag{6}$$

Substituting Eq. (5) in Eq. (6) and replacing $\mathrm{d}T_m/\mathrm{d}x$ with $(T_H - T_C)/\Delta x = \Delta T/\Delta x$ one find for the maximum (steady-state) temperature difference expected across the TAC

$$\begin{aligned}\Delta T \;=\; & \frac{T_m \beta \Delta x}{(1+\varepsilon_s)(1+\sigma)} \\ & \times \mathrm{Im}\left\{\frac{[(1+\sqrt{\sigma})+i(1-\sqrt{\sigma})]}{[1-(1-i)\delta_v/2y_o]} P_1\langle\tilde{u}_1\rangle\right\} \\ & \times \left[\frac{\rho_m c_P[(1+\sigma\varepsilon_s)-\sigma\sqrt{\sigma}(1+\varepsilon_s)]}{\omega(1+\varepsilon_s)(1-\sigma^2)(1-\delta_v/y_o+\delta_v^2/2y_o^2)}\left|\langle u_1\rangle\right|^2 \right. \\ & \left. + \frac{4(y_o K + l K_s)}{\delta_\kappa}\right]^{-1}\end{aligned} \tag{7}$$

where P_1 and $\langle u_1\rangle$ are calculated at the mean position of the stack.

As a TAC may be retained to be acoustically not intrusive, pressure and velocity of the stationary wave can be expressed with the standard formulas [25,26]:

$$P_1 = \frac{i\rho_m\omega}{\gamma'}U_A\frac{\cosh(\gamma' x)}{\sinh(\gamma' L)} \qquad \langle u_1\rangle = U_A\frac{\sinh(\gamma' x)}{\sinh(\gamma' L)} \tag{8}$$

where $\gamma' = ik^* = \alpha + i\beta'$ and where, at a first approximation, the Kirchoff–Rayleigh's formula for sound absorption in wide tubes [3] can be used to evaluate α and β'

$$\alpha = \frac{\omega\delta_v}{2aR}\left[1+(\gamma-1)\frac{\delta_\kappa}{\delta_v}\right] \qquad \beta' = \frac{\omega}{a} + \alpha \tag{9}$$

These equations describe a standing sound wave in a tube of length L closed at the end $x = 0$ with an acoustically hard termination, driven at the end $x = L$ by a piston vibrating with amplitude velocity U_A and resonating for $\beta' L = n\pi$ $(n = 1, 2, 3, \ldots)$ (see Fig. 2).

Anyway, since our measurements involve the acoustic pressure P_A at the driver-end $(x = L)$ it is convenient to rewrite Eqs. (8) in a slightly different form. Observing that the first of Eqs. (8) yields the following relation between P_A and U_A

$$P_A = P_1(x = L) = \frac{i\rho_m\omega}{\gamma'}U_A\frac{\cosh(\gamma' L)}{\sinh(\gamma' L)} \tag{10}$$

Eqs. (8) become

$$P_1 = P_A\frac{\cosh(\gamma' x)}{\cosh(\gamma' L)} \qquad \langle u_1\rangle = \frac{\gamma'}{i\omega\rho_m}P_A\frac{\sinh(\gamma' x)}{\cosh(\gamma' L)} \tag{11}$$

Eq. (7) (or similar) has been extensively employed to compare theory with experiments. These tests have demonstrated that a good agreement exists only at low values of the drive ratio ($DR \leqslant 0.003$) [8,15,27].

3. Experimental apparatus

A sketch of the experimental apparatus is illustrated in Figs. 1 and 2. It consists of a half-wavelength [3] sealed resonator having its fundamental resonance frequency at about 200 Hz. The resonator was built from a straight stainless steel tube of length 0.86 m, internal diameter 7.3 cm and wall thickness 1 mm. The working fluid was air at atmospheric pressure. One extremity of the tube was sealed up by a steel plate 3 cm thick; it constitutes the rigid end (reflector) of the resonator. At the other end a "coupling" steel flange has been fixed to accommodate the mid-range loudspeaker constituting the acoustic power source (driver). A function generator provided with a GPIB interface and a power amplifier has been employed to drive the system at the operation frequency and with the selected power. To reduce as much as possible the heat input coming from the voice coil of the loudspeaker, this last has been cooled by means of an air flow mechanically activated. Pressure measurements were made by a wide dynamic range miniature transducer housed in the coupling flange where a short circular cross section channel has been made to communicate the local pressure to the transducer. This last is thus positioned very near the driver end in correspondence of a pressure antinode. The output signal, opportunely preamplified, has been monitored by a digital memory oscilloscope. Pressure measurements accuracy is estimable about two percent.

The stack was built having care to satisfy the TAC requisites. It consists of five polyethylene plates of thickness 0.6 mm, length 7 cm (much less than the acoustic wavelength $\lambda \approx 1.7$ m), width 5 cm and separated through spacers by 1.1 mm, an amount that is substantially larger than the thermal and viscous penetration depths that, at the involved frequencies, are respectively $\delta_\kappa = 0.19$ mm and $\delta_\nu = 0.16$ mm. The density, heat capacity and thermal conductivity of the plates material, found in literature, are respectively $\rho_s = 1050$ kg·m^{-3}, $c_s = 1200$ J·kg^{-1}·K^{-1} and $K_s = 0.1$–0.13 W·m^{-1}·K^{-1}; from the measured mass/area ratio it resulted $c_A = 844$ J·m^{-2} for the heat capacity per unit area of a stack plate. The TAC was placed in a cylindrical support structure of i.d. 6 cm, length 10 cm and thickness 1 mm; this last has been "suspended" inside the tube by means of thin spacers. Temperature measurements at the extremities H and C of the central plate have been performed with an accuracy of ± 0.1 K by means of two miniature thermo-resistances and two digital multimeters provided with GPIB interface. Thermo-resistances have been inserted within the central plate to minimize their impact on the acoustic field. The other plates ("guard plates" [15]) ac-

complish essentially to the task of reducing the heat flow in the transverse Y direction.

The hermetic seal of the entire apparatus has been guaranteed providing each movable part (closed end plate, coupling flange, etc.) with O-ring seals and fitting any possible gap with vacuum grease. In this way the device can be easily assembled and disassembled to allow a rapid replacement of the TAC inside the resonator.

Taking into account for the reproducibility of the experimental measurements, the overall accuracy of the experimental data is of the order of ten percent.

4. Operation procedure and experimental results

The heating and cooling effects at the stack ends were studied quantitatively recording as a function of time the thermo-resistance signal output when system is driven at its fundamental resonance frequency. This last has been determined in a preliminary phase tuning the frequency at low dynamic pressure until the microphone signal reaches a maximum. Sufficient time is then allowed to pass until every eventual thermal gradient raised inside the TAC is annulled. At the beginning of each set of measurements the entire structure is at room temperature (∼293 K). Next, the forced ventilation for driver refrigeration is started and acoustic power is suddenly applied (at $t = 0$) with the amplifier gain set to the proper level. In order to get information on the dependence of the TAC response on the dynamic pressure amplitude and on the spatial profile of the standing wave, measurements have been performed for different positions of the TAC along the resonator axis and for different gain levels of the audio amplifier.

In Fig. 3 a typical experimental result is shown. Data reported refer to the time variation of the temperatures T_H and T_C, measured at the extremities of the central plate of the TAC, and of their difference $\Delta T = (T_H - T_C)$, for a selected dynamic pressure and for a fixed position of the stack inside the resonator. The temperature difference across the stack increases rapidly in the early stages of the process, where its growth is highest. The trend clearly reflects the increasingly role played by a diffusive heat flow from H to C which tends to balance the hydrodynamic one. As driven by the temperature difference ΔT, this flow is zero at the initial time ($t = 0$), where curves exhibit their maximum slope, and maximum at the steady state, when curves become flat.

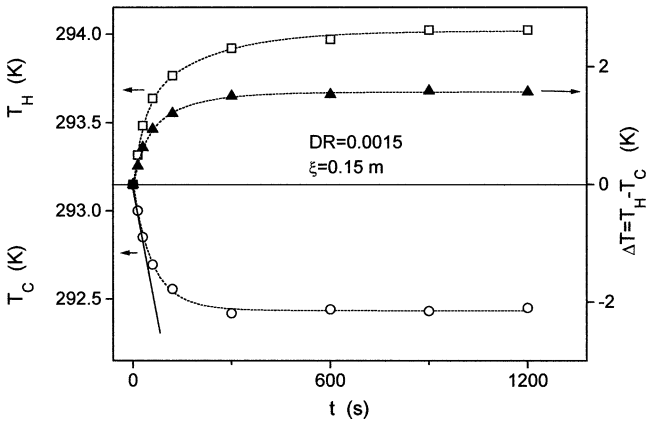

Fig. 3. Time evolution of the measured temperatures at the ends of the central plate of the stack for given values of the drive ratio (*DR*) and of the mean distance of the TAC from the driver end (ξ). Dotted lines are guides for the eye. The straight line is a fit of the experimental T_C data in the first few seconds of the process with a linear law.

In Fig. 4 the measured (points) steady-state temperature difference across the TAC is plotted as a function of ξ, the mean distance of the TAC from the driver end of the resonator, at selected drive ratios P_A/P_m. The dramatic reduction of the heating and cooling effects for $\xi \to L/2 = 0.43$ m reflects the approaching of the pressure node where the TAC response would theoretically be zero. As it results from Eq. (7), in fact, the temperature difference $\Delta T = (T_H - T_C)$ is proportional to the product of particle velocity and acoustic pressure. Therefore, if either of these variables is zero, so must be ΔT. The reduction of the effect is much less intense for $\xi \to 0$ and visible only in the curve at the lowest drive ratio. This trend, not observed in analogue studies [15,22] (where the TAC was positioned near the closed end of the resonator) would be an effect of the approaching of the loudspeaker [28]; in principle, the cross section at $\xi = 0$ would coincide with the oscillating diaphragm of the loudspeaker and, therefore, does not correspond to a velocity node.

5. Analysis and discussion

In Fig. 4 the comparison between the experimental ΔT values (points) and the theoretical ones (lines) is reported. These last have been computed by means of Eq. (7) utilizing

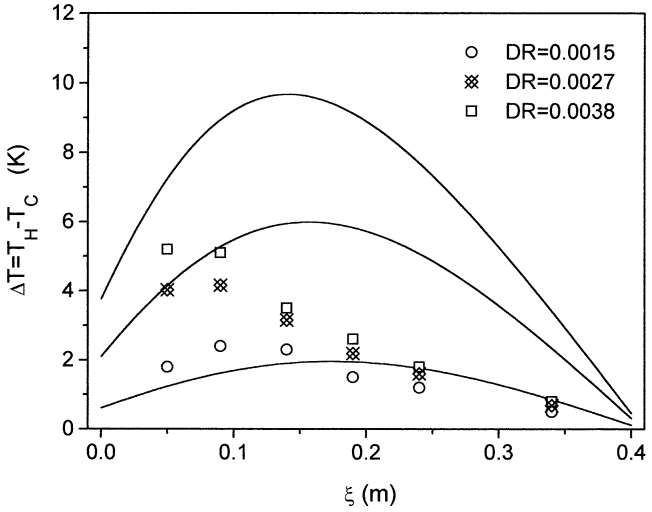

Fig. 4. Measured (points) and theoretical (lines) values of the equilibrium temperature differences along the central plate of the TAC as a function of the mean distance of the TAC from the driver end (ξ) and for selected values of the drive ratio (*DR*).

the known thermo-physical properties of the gas and making use of Eqs. (9) and (11) to evaluate α, β' and the local values of P_1 and $\langle u_1 \rangle$, (P_A and ω being experimentally measured). As it is clearly visible, the measurements agree well with theory only for drive ratios less than approximately two-tenth percent, the agreement being lost at higher *DR* values. The predicted ΔT values, in fact, overestimate the measured ones and the discrepancy grows at increasing the drive ratio. At the highest *DR* shown in Fig. 4 the theoretical values exceed the experimental ones by about forty percent. Each curve approaches the measured data only in proximity of the pressure node and antinode where thermoacoustic effect naturally vanishes. In no case, moreover, theoretical predictions agree with the maximum ΔT location and with the experimental points located around $L/4(\xi \approx 0.2$ m). Eq. (7), however, is able to take into account the observed evolution from a sinusoid to a saw-tooth curve and the shift of the maximum temperature difference towards the pressure antinode, two features also highlighted in references [15] and [22].

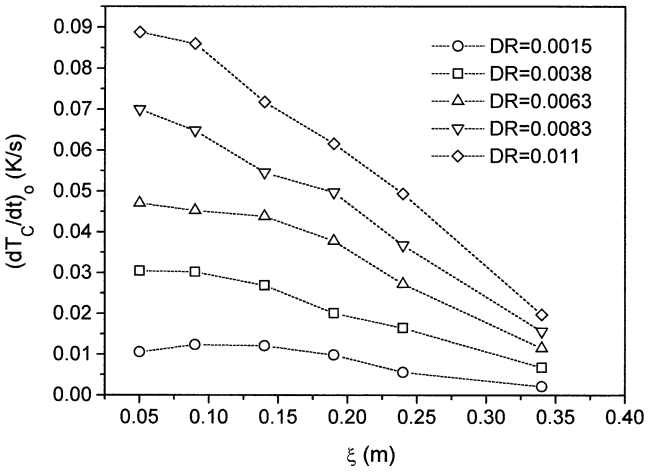

Fig. 5. Measured initial time rate of change of the temperature at the "cold" side (C) of the central plate of the stack as a function of the mean distance of the TAC from the driver end (ξ) and for fixed values of the drive ratio (*DR*). Dotted lines are guides for the eye.

It must be observed, however, that reliability of data suffers (in addition of the experimental uncertainty which, anyway, does not justify the observed deviations) from intrinsic limitations which can be due to the following causes:

(A) non-linear effects (presence of harmonics greater than the fundamental);
(B) turbulent flow, vortex generation, jetting (which can become relevant at the stack ends);
(C) spurious heat leaks from the outside (the resonator tube was not insulated from the surrounding);
(D) heat generated by viscous losses on the resonator walls and carried to the stack by acoustic streaming (this time-averaged convective heat flux constitutes an additional thermal load to the cold end of the stack);
(E) heat fluxes in the transverse Y direction (contrarily to what is assumed by the standard theory of thermoacoustics, the time-average temperature of the fluid could be different from that of the adjacent stack-walls);
(F) heat transfer at the ends of the stack (the hypothesis of a perfectly isolated stack, i.e., one for which no heat is allowed to enter or leave either transversally or axially through the ends, could not hold).

The effect of phenomena labeled with letters (C), (D), (E), (F), is obviously maximum when system is in dynamic equilibrium and minimum during the first few seconds after the sudden application ($t = 0$) of sound to the tube (when temperature is still uniform through the entire system). So, to get quantitative information on the initial time heat flux $(\dot{Q}_2)_0$, the initial time rate of change of the temperature at the cold side of the stack $(\mathrm{d}T_C/\mathrm{d}t)_0$ has been extracted from the temporal measurements. To this end the experimental $T_C(t)$ curves have been fitted with a linear law in the initial times of the process. In fact, during the first few seconds,

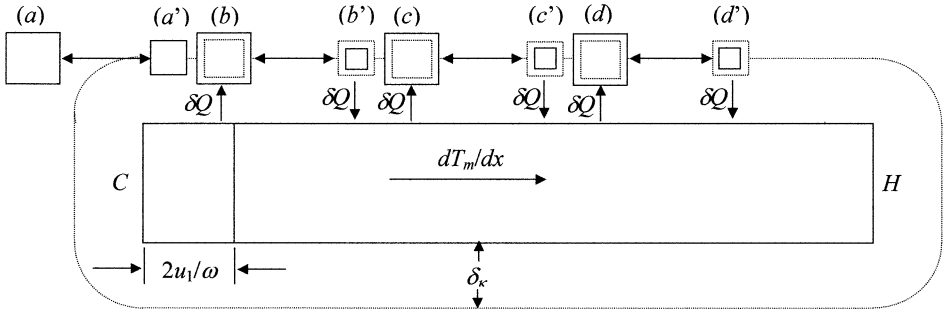

Fig. 6. Magnified illustration of a stack-plate and elementary thermoacoustic cycle. Parcels of gas (boxes) are compressed, expanded and displaced by the acoustic field, and exchange heat with the plate. Boxes labeled with (a) and (a') (and similarly for the other) indicate the same parcel at the extreme positions of its oscillatory motion so (b) takes the place of (a'), (c) takes the place of (b'), etc. At middle positions of the plate the net heat transfer from fluid to plate is zero. In fact, heat δQ extracted from the plate by (c) is reversed to the plate by (b') half acoustic cycle after, heat δQ extracted from the plate by (d) is reversed to the plate by (c') half acoustic cycle after and so on. However, at the stack-ends this conclusion is no more true. Parcel (a'), for example, does not make thermal contact with the plate in the (a) position. So, even if it is cooler by $2T_1$ on moving on (a), it has no means to relax its temperature and does not contribute to the heat flow. The heat absorbed from the plate by (b), therefore, is not compensated and a net quantity of heat is extracted every cycle from the side C of the plate on a distance from the edge equal to $2u_1/\omega$, the peak-to-peak acoustic displacement amplitude.

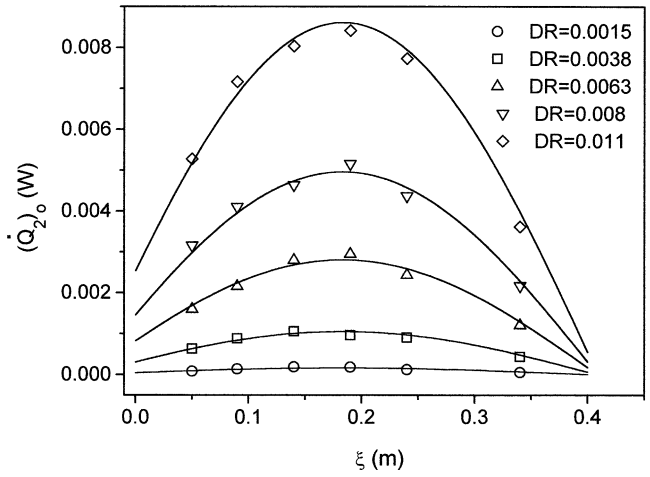

Fig. 7. Experimental (points) and theoretical (lines) values of the initial time convective heat flux along the central plate of the stack as a function of the mean distance of the TAC from the driver end (ξ) and for selected drive ratios (*DR*).

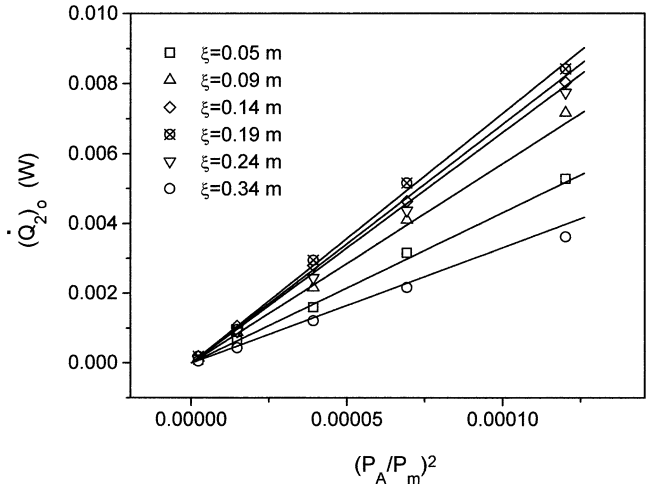

Fig. 8. Experimental (points) and theoretical (lines) values of the initial time convective heat flux along the central plate of the stack as a function of the squared drive ratio $(P_A/P_m)^2$ and for selected (mean) distances of the TAC from the driver end (ξ).

there are no limiting or redistributing mechanisms for the heat flux $\dot{Q}_2$, then the temperature would vary linearly with time, as it can be effectively observed in Fig. 3. The obtained results are shown in Fig. 5.

As a plate is heated (or cooled) on both sides we can write

$$2(\dot{q}_2)_0 = c_A\left(\frac{\mathrm{d}T_C}{\mathrm{d}t}\right)_0 \tag{12}$$

where $(\dot{q}_2)_0$ is the initial time heating rate of the plate per unit area. This last is related to $(\dot{Q}_2)_0$ by the equation

$$(\dot{q}_2)_0 = (\dot{Q}_2)_0\left(\frac{2\Pi u_1}{\omega}\right)^{-1} \tag{13}$$

making the assumption that net extraction of heat occurs at the edge C of each plate from a band wide $2u_1/\omega$, the peak-to-peak acoustic displacement amplitude (see Fig. 6). Substituting this expression into Eq. (12) one finds finally

$$(\dot{Q}_2)_0 = \Pi c_A \frac{u_1}{\omega}\left(\frac{\mathrm{d}T_C}{\mathrm{d}t}\right)_0 \tag{14}$$

The heat flux values $(\dot{Q}_2)_0$, calculated by means of this expression, with all parameters appearing on the right side experimentally measured—u_1 being calculated from the measured P_A through the second of Eqs. (11)—, are plotted in Fig. 7 as a function of ξ at selected *DR* values. The agreement with the theoretical curves calculated by means of Eq. (5) (where now only the first term must be retained as at the initial time of the process $\mathrm{d}T_m/\mathrm{d}x \approx 0$) is fairly good for all the drive ratios examined. Analogously, the plot of the experimental data as a function of $(P_A/P_m)^2$ at fixed ξ, reported in Fig. 8, shows as the dependence of $(\dot{Q}_2)_0$ on $(P_A)^2$, expressed by Eq. (5), is well satisfied.

6. Conclusions

In the present work, on the basis of the linear thermoacoustic theory, a simple calculus procedure has been outlined in order to investigate the origin of the deviations of the predictions of the linear theory from the measured performances of real devices.

The method, relying on a temporal approach, naturally minimizes the incidence on experimental data of time-average heat transfer processes not taken into account by the standard theory. The procedure, therefore, could constitute a complementary to conventional analysis performed for validation of the linear theory.

As for the experimental data presented in this work, it is found that the onset of the deviations observed between the theoretical ΔT values and the experimental ones occurs for drive ratios greater than approximately two-tenth percent. The causes for these irregularities, however, are not found in non linear effects such as the high harmonic content of the pressure oscillations. In effect, for dynamic pressure amplitudes less than one percent of the mean pressure and for acoustic Reynolds numbers ($Re = u_1\delta_\nu/\nu$ [29]) near 50, linear thermoacoustic theory is expected to apply, as is demonstrated by the good agreement found between the rate of change of temperature measurements and the temporal analysis here proposed. On the other hand, as shown in flow-field numerical simulations [30], effects labeled with letter (B) become relevant for *DR* values greater than approximately two percent, well above the range covered in the present investigation. The cause of the disagreement has probably to be found in complexes processes of thermal exchange of the kind labeled with letters (C), (D), (E), (F). In particular, the knowledge of the temperature and flow fields at the edges of the stack plates is fundamental for estimating the local value of the heat exchange coefficient. This information, in turn, could allow to make more reliable theoreti-

cal predictions on the value of the stack equilibrium temperature gradient and to design high efficiency heat exchangers to be connected at the stack ends.

Anyway, the good agreement found between experimental data and temporal analysis seem to validate the hypothesis inherent in Eq. (13) concerning the linear dimension of the stack-plate where net exchange of heat occurs. This result, in turn, could constitute an experimental evidence for the fact that, at least at low drive ratios, the optimum heat exchangers length along the particle displacement direction (X direction) should be of the order of the local peak-to-peak acoustic oscillation amplitude of the fluid particles ($2u_1/\omega$), as previously argued by Swift on heuristic grounds.

A number of modifications are actually carried out on the described prototype. The realization of a high efficiency driver able to deliver at least 8–10 W of acoustic power is fundamental to extend the investigation to higher DR values. Furthermore, it is necessary to establish which one of the causes labeled with letters (A)–(F) was revealed critical in determining the observed deviations. This knowledge is essential to establish which combinations of stack/resonator dimensions and gas parameters optimize the performance of a TAC.

References

[1] C. Sondhauss, Ueber die schallschwingungen der luft in erhitzten glasröhren und in gedeckten pfeifen von ungleicher weite, Ann. Phys. 79 (1850) 1–38.

[2] P. Merkli, H. Thomann, Thermoacoustic effects in a resonance tube, J. Fluid. Mech. 70 (1975) 161–177.

[3] L. Rayleigh, The Theory of Sound, Dover Press, New York, 1945.

[4] N. Rott, Thermoacoustics, Adv. Appl. Mech. 20 (1980) 135–175, and references therein.

[5] G.-W. Swift, Thermoacoustic engines, J. Acoust. Soc. Amer. 84 (1988) 1145–1180.

[6] T. Hofler, Thermoacoustic refrigerator design and performance, Ph.D. Thesis, University of California, San Diego, 1986.

[7] G.-W. Swift, A. Migliori, T. Hofler, J. Wheatley, Theory and calculations for an intrinsically irreversible acoustic prime mover using liquid sodium as working fluid, J. Acoust. Soc. Amer. 78 (1985) 767–781.

[8] A. Migliori, G.-W. Swift, Liquid sodium thermoacoustic engine, Appl. Phys. Lett. 53 (1988) 355–357.

[9] G.-W. Swift, Analysis and performance of a large thermoacoustic engine, J. Acoust. Soc. Amer. 92 (1992) 1551–1563.

[10] S.-C. Ballister, D.-J. McKelvey, Shipboard electronics thermoacoustic cooler, Master of Science Thesis, Physics Department, Naval Post graduate School, 1995, Dtic Report No. ADA 300514; US Patent No. 5, 674, 216 (July 15, 1997).

[11] S.-L. Garrett, J.-A. Adeff, T.-J. Hofler, Thermoacoustic refrigerator for space applications, J. Thermophys. Heat Transfer 7 (1993) 595–599.

[12] S.-L. Garret, D.-K. Perkins, A. Gopinath, Thermoacoustic refrigerator heat exchangers: Design, analysis and fabrication, in: G.F. Hewitt (Ed.), Proceedings of the Tenth International Heat Transfer Conference Brighton, UK, 1994, pp. 375–380.

[13] R. Radebaugh, A review of pulse tube refrigeration, Adv. Cryog. Engen. 35 (1990) 1191–1205.

[14] G.-W. Swift, R. Radebaugh, R.-A. Martin, US Patent No. 4, 953, 366 (1990).

[15] A.-A. Atchley, T.-J. Hofler, M.-L. Muzzerall, M.-D. Kite, C. Ao, Acoustically generated temperature gradients in short plates, J. Acoust. Soc. Amer. 88 (1990) 251–263.

[16] G.-W. Swift, Thermoacoustic engines and refrigerators, Phys. Today, (July) (1995) 22–29.

[17] M. Wetzel, C. Herman, Design optimization of thermoacoustic refrigerators, Internat. J. Refrig. 20 (1997) 3–21.

[18] V.-E. Gusev, H. Bailliet, P. Lotton, S. Job, M. Bruneau, Enhancement of the Q of a nonlinear acoustic resonator by active suppression of harmonics, J. Acoust. Soc. Amer. 103 (1998) 3717–3720.

[19] G. Mozurkewich, A model for tranverse heat transfer in thermoacoustics, J. Acoust. Soc. Amer. 103 (1998) 3318–3326.

[20] G. Mozurkewich, Time average temperature distribution in a thermoacoustic stack, J. Acoust. Soc. Amer. 103 (1998) 380–388.

[21] A. Gopinath, N.-L. Tait, S.-L. Garrett, Thermoacoustic streaming in a resonant channel: The time averaged temperature distribution, J. Acoust. Soc. Amer. 103 (1998) 1388–1405.

[22] J. Wheatley, T. Hofler, G.-W. Swift, A. Migliori, An intrinsically irreversible thermoacoustic heat engine, J. Acoust. Soc. Amer. 74 (1983) 153–170.

[23] J. Wheatley, T. Hofler, G.-W. Swift, A. Migliori, Experiments with an intrinsically irreversible acoustic heat engine, Phys. Rev. Lett. 50 (1983) 499–502.

[24] J. Wheatley, T. Hofler, G.-W. Swift, A. Migliori, Understanding some simple phenomena in thermoacoustics with applications to acoustical heat engines, Amer. J. Phys. 53 (1985) 147–161.

[25] E. Meyer, E.-G. Neumann, Physical and Applied Acoustics, Academic Press, New York, 1972.

[26] I.-C. Romer, R.-A. Gaggioli, A.-S. El-Hakeem, Analysis of Quadripole methods for the velocity of sound, J. Acoust. Soc. Amer. 40 (1966) 86–98.

[27] J.-R. Olson, G.-W. Swift, Similitude in thermoacoustics, J. Acoust. Soc. Amer. 95 (1994) 1412.

[28] R.-S. Wakeland, Use of electrodynamic drivers in thermoacoustic refrigerators, J. Acoust. Soc. Amer. 9107 (2000) 827–832.

[29] P. Merkli, H. Thomann, Transition to turbulence in oscillating pipe, J. Fluid Mech. 68 (1975) 567–579.

[30] A.-S. Worlikar, O.-M. Knio, R. Klein, Numerical simulation of a thermoacoustic refrigeration, J. Comput. Phys. 144 (1998) 299–324.